J Nanopart Res (2011) 13:2099–2107
DOI 10.1007/s11051-010-9967-5

RESEARCH PAPER

Dendrimer-conjugated magnetic nanoparticles for removal of zinc (II) from aqueous solutions

Chih-Ming Chou · Hsing-Lung Lien

Received: 3 September 2009 / Accepted: 16 May 2010 / Published online: 30 May 2010

Abstract Dendrimers are novel nanostructure materials that possess a unique three-dimensional molecular configuration. They have high adsorption capacities of heavy metals. Dendrimer-conjugated magnetic nanoparticles (Gn-MNPs) combining the superior adsorbent of dendrimers with magnetic nanoparticles (MNPs) have been developed for effective removal and recovery of Zn(II). In this study, the Gn-MNPs were synthesized, characterized, and examined as reusable adsorbents of Zn(II). Characterization conducted by transmission electron microscopy (TEM), X-ray diffraction (XRD), Fourier transform infrared spectroscopy (FTIR), and elemental analysis revealed that dendrimers were successfully coated onto the surface of MNPs made of magnetite (Fe_3O_4). The pH effect studies indicate the Zn(II) adsorption with Gn-MNPs is a function of pH. The adsorption efficiency increases with increasing pH. At pH less than 3, Zn(II) is readily desorbed. Hence, the Gn-MNPs can be regenerated using the diluted HCl aqueous solution (0.1 M) where Zn(II) can be recovered in a concentrated form. It was found that the Gn-MNPs underwent 10 consecutive adsorption–desorption processes still retained the original removal capacity of Zn(II). The adsorption data were fitted well with both Langmuir and Freundlich isotherms. The maximum adsorption capacity determined by the Langmuir model is 24.3 mg/g at pH 7 and 25°C. A synergistic effect between the complexation reaction and the electrostatic interaction may account for the overall performance of Gn-MNPs.

Keywords Dendrimer · Magnetic nanoparticles · Magnetite · Heavy metals · Adsorption · Removal and recovery of Zn

C.-M. Chou · H.-L. Lien (✉)
Department of Civil and Environmental Engineering, National University of Kaohsiung, 811 Kaohsiung, Taiwan, Republic of China
e-mail: lien.sam@nuk.edu.tw

Introduction

Poly(amidoamine) (PAMAM) dendrimers are a new class of nanomaterials with three-dimensional structure. The highly branched polymers consisted of three basic units including an ethylenediamine core, repeating units, and terminal units (Zeng and Zimmerman 1997; Newkome et al. 2001; Crooks et al. 2001). PAMAM dendrimers are synthesized through a serial repetition of two reactions: Michael addition reaction of amino groups to the double bond of methyl acrylate, followed by amidation of the resulting methyl ester with ethylene diamine (Zeng and Zimmerman 1997). The first iteration of these two reactions results in the formation of zero-generation dendrimer (G0). The subsequent cycles of each addition-amidation reaction lead to produce a higher generation dendrimer. Dendrimers with amine-terminated functional groups

are called full-generation dendrimers. The diameter of PAMAM dendrimers increases by roughly 1 nm per generation. For example, the diameter of G3 and G5 PAMAM is 2.9 and 4.5 nm, respectively (Crooks et al. 2001).

The use of PAMAM dendrimers for environmental applications has been reported for the adsorptive removal of heavy metals from water and soil (Diallo et al. 1999, 2005; Xu and Zhao 2005). Amine-terminated PAMAM dendrimers exhibit a high binding affinity for metal ions to their surface via coordination to the amine or acid functionality (Crooks et al. 2001). As the complexation of metal ions with the dendrimer is pH-dependent, the release of metal ions from dendrimers can be readily achieved by the protonation of amine functional groups at low pH (Crooks et al. 2001). The adsorbed ions can therefore be recovered in a concentrated form for disposal or reuse. This feature makes PAMAM dendrimers particularly promising as reusable chelating agents for the metal ion separation. Recently, the ultrafiltration was applied to recover dendrimers (Diallo et al. 2005). Although studies have showed that the PAMAM dendrimers have low tendency to foul cellulose membranes (Diallo et al. 2005), fouling is still one of the main problems in any membrane separation (Van der Bruggena et al. 2008). Hence, there is a need to develop methods for effective separation and recovery of dendrimers.

Magnetic separation has been considered as an effective method for solid–liquid phase separation techniques and has been applied to the wastewater treatment and environmental pollution control (Hattori et al. 2002; Lo et al. 2009). For example, the use of magnetic-activated sludge with the application of an external magnetic field has been developed in the wastewater treatment (Hattori et al. 2002). Iron-based magnetic nanoparticles (MNPs) with large surface areas such as nanoscale magnetite (Fe_3O_4) have been shown to be good adsorbents for removal of heavy metals because of their high adsorption capacity, short adsorption time, and the easy separation of metal ion laden MNPs by applying an external magnetic field (Ngomsik et al. 2005). The magnetic separation minimizes the production of the secondary waste caused by the nanoparticles themselves. In principle, the adsorbent should be regenerated for reuse; however, the interactions between the iron oxide and metal ions involving chemisorption or surface chemical reactions are often irreversible (Clifford and Ghurye 2002; Hu et al. 2004; Lien and Wilkin 2005; Yavuz et al. 2006). As a result, the regeneration of this kind of adsorbent may be limited.

In this study, we present dendrimer-conjugated magnetic nanoparticles (Gn-MNPs, n: dendrimer generation number) combining the adsorption/desorption with magnetic separation for the removal and recovery of Zn(II) from aqueous solutions. The Gn-MNPs make dendrimers readily to be recovered and reused while the adsorbed ions can easily be concentrated. Magnetite nanoparticles were chosen as magnetic supports because they can simply be synthesized in large quantity (Mehta et al. 1997) while zinc ion was selected as the target contaminant. Industries including galvanizing plants, zinc and brass metal works, and natural ores discharge waste streams containing significant levels of zinc (Norton et al. 2004). Like many other metals such as arsenic, copper, cadmium, lead, and mercury, zinc is toxic and commonly detected in the environments. World Health Organization (WHO) reported that the drinking water containing zinc at levels above 3 mg/L can cause an undesirable astringent taste (WHO 2003). The United States Environmental Protection Agency (USEPA) has set a maximum allowable level of zinc at 5 mg/L in National Secondary Drinking Water Regulations (USEPA 2001).

In this article, the objective is aimed at investigating the feasibility of using Gn-MNPs as reusable adsorbents for the removal and recovery of Zn(II) in water. The size, structure, and surface properties of Gn-MNPs were characterized by transmission electron microscopy (TEM), X-ray diffraction (XRD), Fourier transform infrared (FTIR) spectroscopy, and elemental analysis. Repetitive adsorption–desorption studies were used to evaluate the reusability of Gn-MNPs.

Experimental section

Materials

All chemicals were reagent grade or above and used without further purification. Ferric chloride ($FeCl_3 \cdot 6H_2O$) and ferrous sulfate ($FeSO_4 \cdot 7H_2O$) were purchased from SHOWA. Zinc chloride, 3-aminopropyltrimethoxysilane ($H_2N(CH_2)_3Si(OCH_3)_3$, APTS),

ethylenediamine ($NH_2CH_2CH_2NH_2$), methanol, ethyl alcohol, ammonium hydroxide, and methylacrylate ($C_4H_6O_2$) were obtained from Aldrich.

Preparation of magnetic nanoparticles

Magnetite nanoparticles were prepared by co-precipitating Fe(II) and Fe(III) ions with ammonia solution and treated under hydrothermal conditions (Mehta et al. 1997). A Fe(III) and Fe(II) mixture solution containing 2.7 g $FeSO_4{\cdot}7H_2O$ and 5.7 g $FeCl_3{\cdot}6H_2O$ (molar ratio Fe(III)/Fe(II) = 2) was dissolved into 100 mL deoxygenated water. Chemical precipitation was achieved by dropwise adding NH_4OH solution (29.3%) to reach pH 10 at 25°C under vigorous stirring. The black precipitates were heated at 80°C for 30 min and were washed several times by deionized water and dried by N_2.

Preparation of dendrimer-conjugated magnetic nanoparticles

Dendrimer-conjugated magnetic nanoparticles were prepared based on the method of Pan et al. (2005) and Gan et al. (2005). A 200 mL ethanol mixture containing 2 g MNPs was placed in a round-bottom flask with a condenser. 10 mL APTS ($H_2N(CH_2)_3Si(OCH_3)_3$) was added and stirred at 60°C for 7 h. The colloids were washed by methanol and dried at room temperature by N_2. The APTS-modified MNPs (2 g), denoted as G0-MNPs, were dispersed in 50 mL methanol with 20 mL methacrylate. The solution was ultrasonicated for 7 h at room temperature. The colloids were washed with methanol 5 times; then, 4 mL ethylenediamine and 20 mL methanol were added and the mixture was stirred for 3 h at room temperature. After washed with methanol 5 times, the first generation dendrimer-conjugated magnetic nanoparticles (G1-MNPs) were produced. The Gn-MNPs with different generations can therefore be achieved by repeating the procedure of adding methacrylate and ethylenediamine.

Batch tests

Adsorption experiments were carried out in a 250 mL high density poly(ethylene), HDPE, vessel containing Gn-MNPs with Zn(II) in 100 mL aqueous solution at 25 ± 1°C. The vessel was placed on a rotary shaker at 170 rpm. The solution pH was adjusted by 1 M HCl or NaOH at the beginning of the reaction and monitored periodically throughout the experiment. Adsorption isotherm studies were conducted by varying the initial Zn(II) concentration from 0.15 mM (10 mg/L) to 0.76 mM (50 mg/L) and the metal loading from 0.5 to 5.0 g/L at neutral pH. Repetitive adsorption–desorption studies of Zn(II) were carried out to evaluate the regeneration of Gn-MNPs. For each cycle, 0.30 mM Zn(II) solution was added in 100 mL aqueous solutions in the presence of 0.1 g G3-MNPs. After the adsorption reached equilibrium, G3-MNPs were separated via an external magnetic field and the desorption was conducted by mixing 0.1 g Zn(II)-laden G3-MNPs with 10 mL of the HCl solution (0.1 M) for 30 min. After the Zn(II) desorption, the regenerated adsorbent was magnetically collected and washed thoroughly with deionized water for adsorption in the succeeding cycle. Identical experiments were conducted using magnetite nanoparticles as a control.

Zinc ion analysis

Analysis of zinc ions was conducted by using an inductively coupled plasma-optical emission spectrometry (ICP-OES, PerkinElmer Optima 2000DV, Perkin Elmer Inc.). The wavelength of Zn(II) was set at 206.219 nm. Prior to analysis, samples were filtered through 0.2-μm filters and acidified with 0.48 M HNO_3. The Zn(II) concentration determined by ICP is the result of triplicate analysis with relative standard deviation less than 1%. Analyses of duplicate samples indicated a relatively analytical error of less than 5% for metal concentrations.

Characterization

Transmission electron microscopy analysis was carried out using a field emission transmission electron microscope (Hitachi Model HF-2000) at 120 kV equipped with energy-dispersive X-ray (EDX). The sample was obtained by placing a drop of the colloid solution onto a Formvar-covered copper grid and evaporated in air at room temperature. XRD measurements were performed on a X-ray diffractometer (Siemens D5000) using Cu K_α radiation producing X-ray with a wavelength of 1.54056 Å. Samples were scanned from 20° to 80° (2θ) at a rate of 2° 2θ/min. Fourier transform infrared spectra (FTIR) were

recorded on a Spectrum GX FTIR spectrometer (Perkin Elmer Inc.). Specific surface areas of Gn-MNPs and MNPs were determined by Brunauer–Emmett–Teller (BET) N_2 method using a COULTER SA 3100 surface area analyzer (Coulter Co.). Analysis of the specific surface area of nanoparticles was conducted in triplicate. The contents of carbon and nitrogen were measured by Elementar vario EL III CHNOS elemental analyzer.

Results and discussion

Characterization of Gn-MNPs

Figure 1 shows the morphology of MNPs and G3-MNPs. An agglomeration of MNPs was observed in the absence of stabilizers due to the lack of any repulsive force between the MNPs (Fig. 1a). The TEM image revealed that MNPs synthesized in this study were multidispersed. However, G3-MNPs were well dispersed in the solution (Fig. 1b). Dendrimers have been widely used as templates for the synthesis of well-dispersed nanoparticles (Crooks et al. 2001). In general, the dispersion methods of nanoparticles include electrostatic stabilization, steric stabilization, and a combination (electro-steric) of the two (Sun 2006). As a result, the well-dispersed G3-MNPs can be attributed to the three-dimensional structure of dendrimers resulted in the steric stabilization. Furthermore, the mean particles size of G3-MNPs is about 10 nm (Fig. 1b), which is consistent with the study of Pan et al. (2005).

Transmission electron microscopy-energy-dispersive X-ray results (Fig. 2) show the presence of silicon at the surface of G3-MNPs suggesting that the aminosilanization was successfully achieved during the preparation. It should be noted that the aminosilanization resulted in the decrease of surface areas and the pore volume. As shown in Table 1, the specific surface area decreased from 97.4 m^2/g before treatment to 68.9 m^2/g after aminosilanization indicating that aminosilanes were anchored onto the inner pore volume of MNPs. This can be confirmed by the decrease in the pore volume of nanoparticles from 0.237 to 0.160 mL/g after aminosilanization. Similar results have also been observed in the aminosilanization of other nanoparticles such as titanium oxide

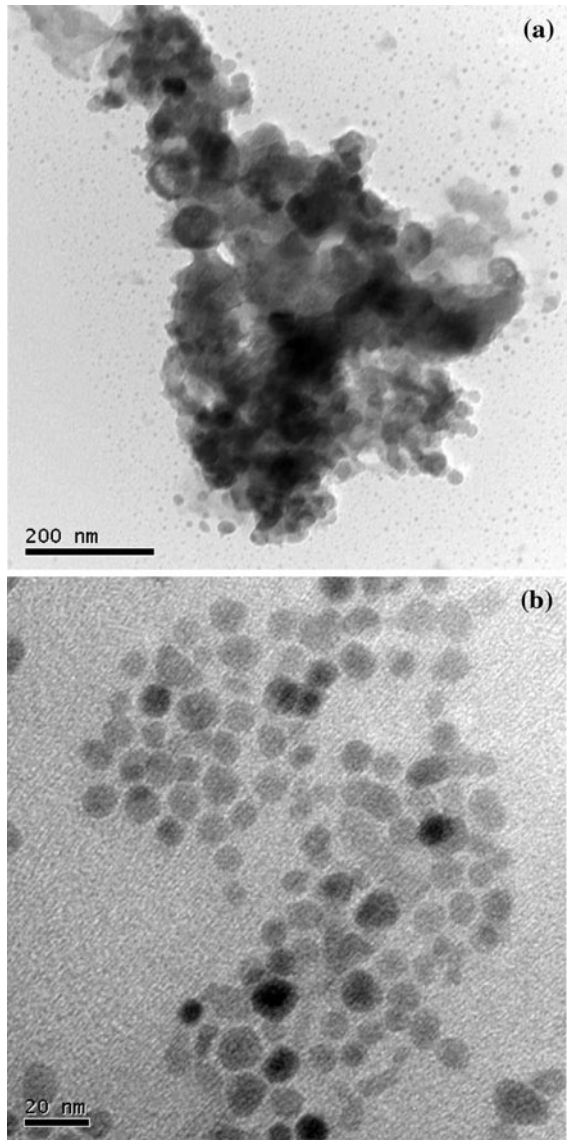

Fig. 1 TEM images of **a** MNPs (magnetite nanoparticles) and **b** G3-MNPs

(Andrzejewska et al. 2004; Ye et al. 2007). Results of XRD analysis are shown in Fig. 3. All the samples exhibited the same XRD pattern. Six characteristic peaks (2θ) at 30.1°, 35.5°, 43.1°, 53.4°, 57.0°, and 62.6° matched well with the standard spectrum of magnetite. This revealed that the dendrimer modification did not alter the properties of MNPs. Furthermore, the grain size of MNPs can be estimated from the XRD analysis using the Scherrer's equation (Cullity and Stock 2001):

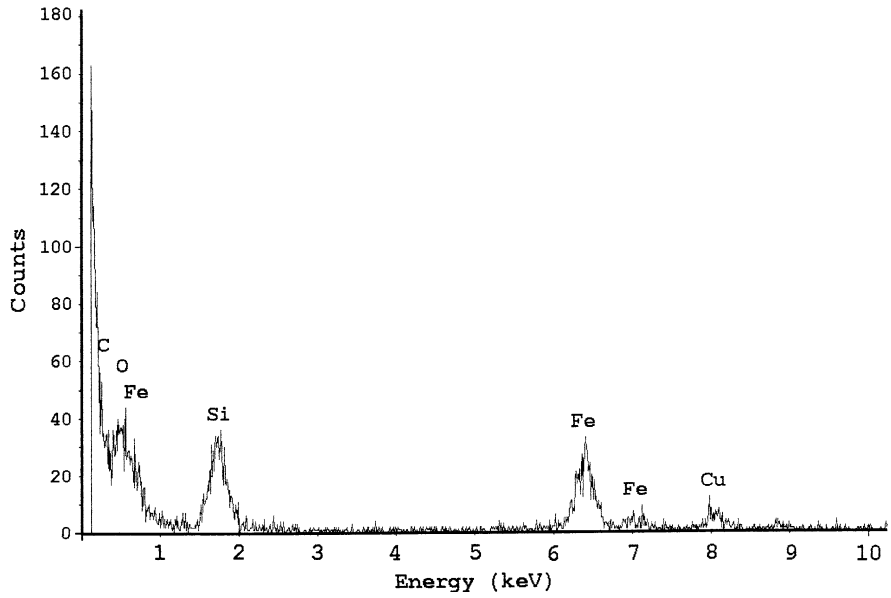

Fig. 2 TEM-EDX of G3-MNPs. Silicon, iron, and oxygen elements were observed

$$d = \frac{0.89 \times \lambda}{B \times \cos \theta_B} \quad (1)$$

where d is the grain size (Å), λ is 1.54056 Å, B is the full width at half-maximum (FWHM), and θ_B is Bragg angle. Based on the XRD patterns shown in Fig. 3, the grain size was calculated to be about 12.7 nm. It should be aware that an error for the grain size by Scherrer's equation can be up to 50%. Nevertheless, this estimation is consistent with the results of TEM (Fig. 1).

The FTIR spectra of MNPs and Gn-MNPs with different generations are illustrated in Fig. 4. A characteristic adsorption band at 579 cm^{-1} attributed to the Fe–O bond of magnetite was observed in all four samples (Pan et al. 2005; Gan et al. 2005). The Gn-MNPs possess absorption bands in 1096.9 and 1010.1 cm^{-1} due to Si–O–Si and Si–O–Fe bonds (Mikhailik et al. 1991; Xu et al. 1997; Li and Bu 2004; Wapner and Grundmeier 2005), which were not found in the spectrum of MNPs. This provides further evidence to confirm the aminosilanization

Table 1 Specific surface area and pore volume of synthesized nanoparticles

Adsorbents	Specific surface area (m^2/g)	Pore volume (mL/g)
MNPs	97.4	0.237
G3-MNPs	56.9	0.160

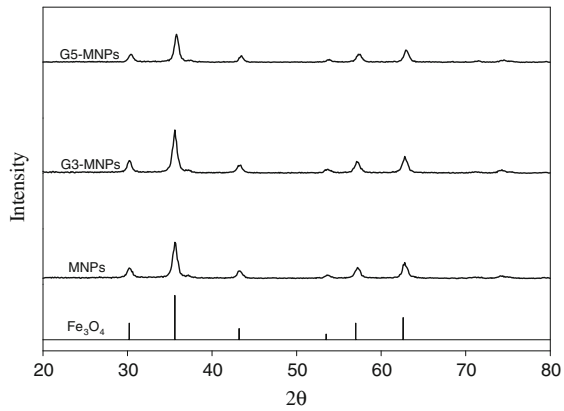

Fig. 3 XRD patterns of MNPs and Gn-MNPs with different generations

reaction was successfully achieved during the preparation. The bending vibration of $–NH_2$ group is at 3440 cm^{-1} and that of the –CO–NH– group is at 1650 and 1555 cm^{-1}, which is in agreement with the studies of Pan et al. (2005) and Gan et al. (2005). However, the molecular water for a broad band at 3400 and 1650 cm^{-1} may mask the signal of $–NH_2$ and –CO–NH– groups, respectively. Nevertheless, as the dendrimer generation increased, the signal intensity increased at 1555 cm^{-1} due to the –CO–NH– group and at 2926 cm^{-1} due to the CH_2– group, respectively. In addition, the elemental analysis revealed that the element of nitrogen, carbon and

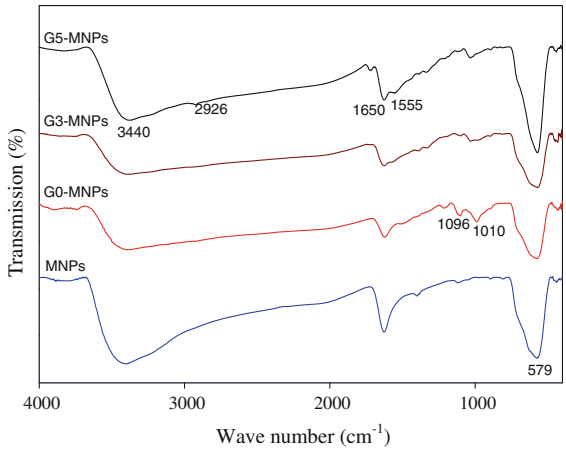

Fig. 4 FTIR spectra of MNPs and Gn-MNPs with different generations

hydrogen accounted for 3.12 ± 0.06, 5.03 ± 0.23, and 1.69 ± 0.13% by weight, respectively, of the total mass of G3-MNPs. No nitrogen and carbon were detected for the MNPs. All these confirm that dendrimers were present and bound to the surface of MNPs.

Removal of Zn(II)

Removal of Zn(II) using various adsorbents at pH 7 is shown in Fig. 5. The initial concentration of Zn(II) was 0.76 mM, and the metal loading was 5.0 g/L. The maximum removal efficiency was only 30% in the presence of MNPs alone while the G3-MNPs and G5-MNPs showed the removal efficiency up to 80%. This indicated that the coating of dendrimers onto the MNP surface enhanced the Zn(II) uptake ability. In general, PAMAM dendrimers have a high binding affinity for metal ions to their surface via the complexation reaction including Cu(II), Fe(III), Ag(I), and Zn(II) (Vassilev and Ford 1999; Crooks et al. 2001; Kaczorowska and Cooper 2009). However, unlike Cu(II) complex coordinated via both core tertiary amines, studies have reported that Zn(II) is either not or weakly bound to the core of the dendrimer. On the other hand, an electrostatic attraction between Zn(II) and the negatively charged surface of Gn-MNPs may be involved in the enhancement of the Zn(II) uptake ability. It has been reported that the iso-electric point of G3-MNPs and G5-MNPs was at pH 6.3 and 6.1, respectively (Pan et al. 2005). As a result, a favorable condition was established for the Zn(II) adsorption by G3-MNPs at pH 7 where the surface of G3-MNPs was negatively charged.

The electrostatic effect on the adsorption of Zn(II) by Gn-MNPs was further confirmed by the study of pH effects. As shown in Fig. 6, the Zn(II) adsorption on the solids increased with increasing pH. At pH 7, G3-MNPs adsorbed maximum amounts of Zn(II). However, only approximately 15 and 22% removal efficiency were achieved at pH 4 and 5, respectively. This shows that the electrostatic interaction may play a role in the adsorption of Zn(II) onto the surface of Gn-MNPs. Similar results have been found in the studies of heavy metal removal using iron-based

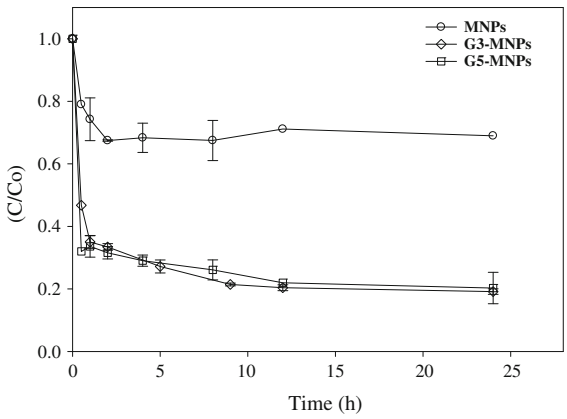

Fig. 5 Adsorption of 0.76 mM (50 mg/L) Zn(II) using various adsorbents at pH 7. The metal loading was 5.0 g/L. Data points and error bars represent the average of triplicate samples and standard deviation, respectively

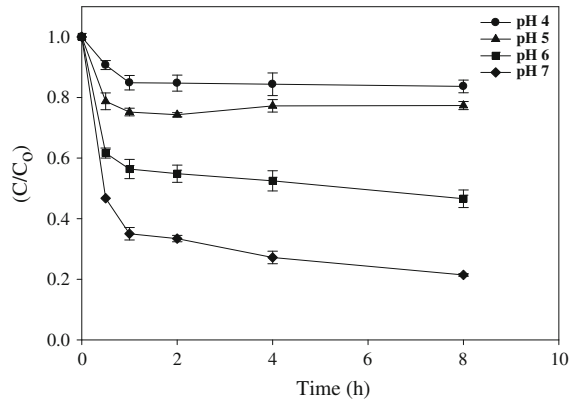

Fig. 6 Effects of pH on the removal of Zn(II) by G3-MNPs. The initial concentration of Zn(II) and the metal loading were 0.15 mM and 1.0 g/L, respectively. Data points and error bars represent the average of triplicate samples and standard deviation, respectively

nanoparticles (Yuan and Lien 2006; Hu et al. 2005). Taken together, a synergistic effect between the complexation reaction and the electrostatic attraction may account for the overall performance of Gn-MNPs. It should be pointed out that there is no significant difference between G3-MNPs and G5-MNPs in terms of the Zn(II) removal efficiency. In fact, Xu and Zhao (2005) reported that dendrimers of lower generation exhibited better removal efficiency of soil-sorbed Cu(II) than those of higher generation. This may be attributed to the reduction of the accessibility of the binding sites caused by the increase of the dendrimer generation. As the dendrimer generation increased, the exterior surface became tighter and the globular shape turned more rigid that may reduce the metal ion access to the dendrimer core.

Adsorption isotherms

Adsorption isotherms of G3-MNPs for zinc ions at 25°C were examined using Langmuir and Freundlich models:

$$q_e = \frac{q_{max} C_e}{1 + aC_e} \quad (2)$$

$$q_e = K_f C_e^{1/n} \quad (3)$$

where q_e is the amount of Zn(II) adsorbed at equilibrium in mg/g, C_e is the solute equilibrium concentration in mg/L, q_{max} and a are Langmuir constants indicating the saturated capacity of adsorbents and an energy term, respectively, and K_f and $1/n$ are the Freundlich constants related to the adsorption capacity and the adsorption intensity, respectively. As shown in Fig. 7, the experimental data correlated well with both the Langmuir and Freundlich equations. The correlation coefficients (R^2) of Langmuir and Freundlich models are 0.957 and 0.953, respectively. The values of q_{max}, a, K_f, and $1/n$ obtained from both models are presented in Table 2. The value of $1/n$ less than 1 indicated that the adsorption of Zn(II) on G3-MNPs was favorable (Ebner et al. 1999). The maximum adsorption capacity determined by the Langmuir model is 24.3 mg/g. Although a direct comparison of G3-MNPs with other adsorbents is difficult due to the different experimental conditions, it was found that the adsorption capacity of G3-MNPs for Zn(II) is generally comparable with other nanoadsorbents at pH 7 and 25°C. For example, the Zn(II) adsorption capacity of powder-activated carbon, β-FeOOH (akaganéite) nanoparticles, multi-walled carbon nanotubes, and single-walled carbon nanotubes was 13.4, 27.61, 32.68, and 43.66 mg/g, respectively (Deliyanni et al. 2007; Lu and Chiu 2006).

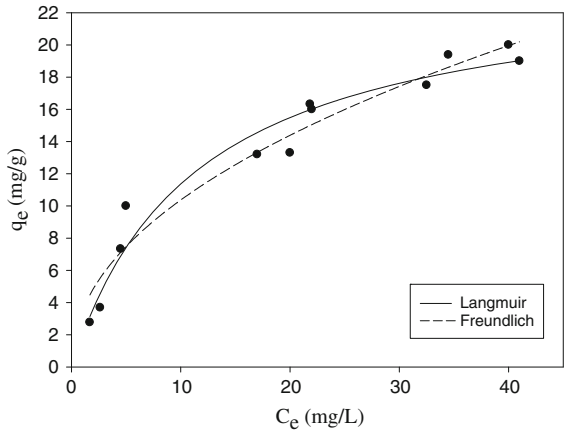

Fig. 7 Adsorption isotherms of Zn(II) by G3-MNPs fitted with Langmuir and Freundlich equations at pH 7

Table 2 Constants of Langmuir and Freundlich models for adsorption of Zn(II) onto G3-MNPs

Langmuir model			Freundlich model		
q_{max}	a	R^2	K_f	$1/n$	R^2
24.30	0.088	0.957	3.49	0.47	0.953

Regeneration studies

To determine the reusability of G3-MNPs, adsorption–desorption experiments were conducted by repetitive spiking of Zn(II) into a batch bottle in 10 consecutive cycles. The regeneration of the G3-MNPs was readily carried out by mixing the Zn(II)-laden G3-MNPs with 10 mL of 0.1 M HCl solution where Zn(II) was recovered in a concentrated form. Figure 8a shows the results of an experiment during which Zn(II) (0.3 mM) was repeatedly spiked into a 250 mL batch bottle containing 1.0 g/L of G3-MNPs powder. It was observed that Zn(II) was rapidly removed in each cycle, and the recovery of

Zn(II) has an average greater than 90% in 10 cycles except for an unexpected decrease at cycle 6. This suggests that the binding sites on the surface of the adsorbent are reversible. On the contrary, the use of MNPs alone for repetitive adsorption–desorption experiments showed a poor performance in terms of the Zn(II) recovery and the regeneration ability of the adsorbent. As shown in Fig. 8b, the Zn(II) removal efficiency decreased significantly by using regenerated MNPs. The average removal efficiency of Zn(II) was about 58% and the average recovery of Zn(II) was only 38% within 8 cycles. Although the variation range among each cycle was relatively large for both Zn(II) removal efficiency and recovery ratio, it is clear that a tendency of inefficient Zn(II) desorption by MNPs was found. This suggests that the interactions between the iron oxide and Zn(II) are mainly irreversible, which is consistent with other studies using magnetite or iron nanoparticles for heavy metal removal (Clifford and Ghurye 2002; Hu et al. 2004; Yavuz et al. 2006). The used G3-MNPs were collected by an external magnet, and more than 75% of the total G3-MNPs can still be recovered after 10 consecutive cycles.

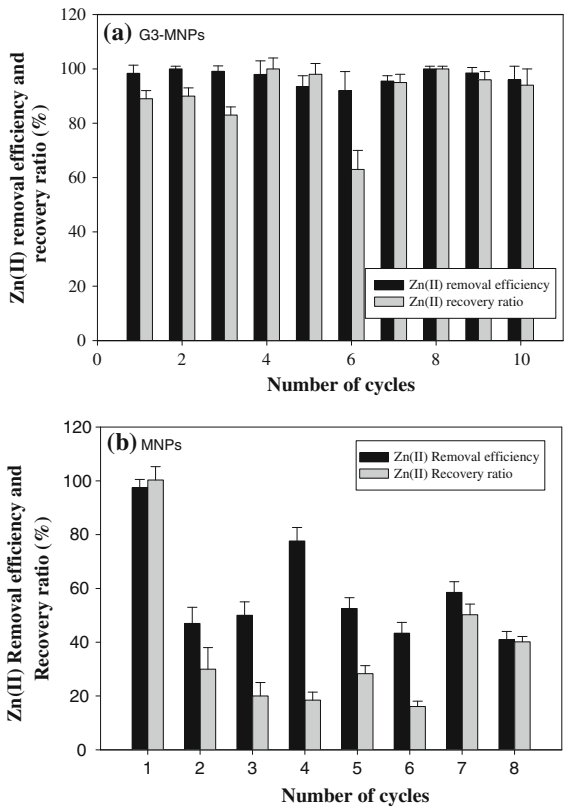

Fig. 8 Repetitive adsorption and desorption of Zn(II) by **a** G3-MNPs and **b** MNPs at pH 7. For each cycle, 0.30 mM Zn(II) was employed and the metal loading was 1.0 g/L. Data points and error bars represent the average of duplicate samples and standard deviation, respectively

Conclusions

Dendrimer-conjugated magnetic nanoparticles have been demonstrated as regeneratable adsorbents capable of effectively removing Zn(II) from aqueous solutions. The Gn-MNPs can be effectively recovered by applying an external magnetic field. In this study, more than 75% of the total G3-MNPs were recovered after 10 consecutive cycles. The adsorption of Zn(II) onto the Gn-MNPs is highly dependent on pH. An increase in pH leads to increase the Zn(II) adsorption efficiency. At pH less than 3, Zn(II) is easily desorbed. As a result, regeneration of Gn-MNPs can be readily achieved using small amounts of 0.1 M HCl solution and Zn(II) can be concentrated for recycling or disposal. The repetitive adsorption and desorption studies indicated that Zn(II) was rapidly removed by G3-MNPs in each cycle, and the recovery of Zn(II) has an average greater than 90% in 10 cycles. Adsorption isotherms were fitted well with both Langmuir and Freundlich models. The maximum adsorption capacity determined by the Langmuir model is 24.3 mg/g, which is generally comparable with other nanoadsorbents at pH 7 and 25°C. A synergistic effect between the complexation reaction and the electrostatic interaction may be involved in the Zn(II) adsorption with Gn-MNPs. This study demonstrates the potential application of Gn-MNPs for removal and recycle of metal ions from water. However, further studies including the selectivity and competitive adsorption of metal ions, effects of the ionic strength and the matrix (e.g., humic substance) effect are needed, before Gn-MNPs can be fully optimized for environmental applications.

Acknowledgments The authors would like to thank the National Science Council (NSC), Taiwan, R.O.C. for the financial support under Grant no. NSC 98-2221-E-390-008-MY3.

References

Andrzejewska A, Krysztafkiewicz A, Jesionowski T (2004) Adsorption of organic dyes on the aminosilane modified TiO_2 surface. Dyes Pigments 62:121–130

Clifford DA, Ghurye GL (2002) Metal-oxide adsorption, ion exchange, and coagulation-microfiltration for arsenic removal from water. In: Frankenberger WT Jr (ed) Environmental chemistry of arsenic. Marcel Dekker Inc, New York, pp 217–245

Crooks RM, Zhao M, Sun L, Chechik V, Yeung LK (2001) Dendrimer-encapsulated metal nanoparticles: synthesis, characterization, and applications to catalysis. Acc Chem Res 31:181–190

Cullity BD, Stock SR (2001) Elements of X-ray diffraction, 3rd edn. Prentice Hall

Deliyanni EA, Peleka EN, Matis KA (2007) Removal of zinc ion from water by sorption onto iron-based nanoadsorbent. J Hazard Mater 141:176–184

Diallo MS, Balogh L, Shafagati A, Johnson JH Jr, Goddard WA, Tomalia DA (1999) Poly (amidoamine) dendrimer: a new class of high capacity chelating agents for Cu(II) ions. Environ Sci Technol 33:820–824

Diallo MS, Christie S, Swaminathan P, Johnson JH Jr, Goddard WA (2005) Dendrimer enhanced ultrafiltration. 1. Recovery of Cu(II) from aqueous solutions using PAMAM dendrimers with ethylene diamine core and terminal NH_2 groups. Environ Sci Technol 39:1366–1377

Ebner AD, Ritter JA, Ploehn HJ, Kochen RL, Navratil JD (1999) New magnetic field-enhanced process for the treatment of aqueous wastes. Sep Sci Technol 34:1277–1285

Gan F, Pan BF, Zheng WM, Ao LM, Gu HC (2005) Study of streptavidin coated onto PAMAM dendrimer modified magnetic nanoparticles. J Magn Magn Mater 293:45–54

Hattori S, Watanabe M, Sasaki K, Yasuharu H (2002) Magnetization of activated sludge by an external magnetic field. Biotechnol Lett 24:65–69

Hu J, Lo MC, Chen GH (2004) Adsorption of Cr(VI) by magnetite nanoparticles. Water Sci Technol 50:139–146

Hu J, Chen G, Lo IMC (2005) Removal and recovery of Cr(VI) from wastewater by maghemite nanoparticles. Water Res 39:4528–4536

Kaczorowska MA, Cooper HJ (2009) Electron capture dissociation and collision-induced dissociation of metal ion (Ag^+, Cu^{2+}, Zn^{2+}, Fe^{2+}, and Fe^{3+}) complexes of polyamidoamine (PAMAM) dendrimers. J Am Soc Mass Spectrom 20:674–681

Li R, Bu JA (2004) Study on the reaction kinetics of dendrimerization by FT-IR spectroscopy: propagation of PAMAM dendrimer on silica gel. Korean J Chem Eng 21:98–103

Lien HL, Wilkin R (2005) High-level arsenite removal from groundwater by zero-valent iron. Chemosphere 59: 377–386

Lo IMC, Hu J, Chen G (2009) Iron-based magnetic nanoparticles for removal of heavy metals from electroplating and metal-finishing waste water. In: Zhang TC, Surampalli RY, Lai KCK, Hu Z, Tyagi RD, Lo IMC (eds) Nanotechnologies for water environment applications, 1st edn. American Society of Civil Engineers (ASCE), USA, pp 213–268

Lu C, Chiu H (2006) Adsorption of zinc(II) from water with purified carbon nanotubes. Chem Eng Sci 61:1138–1145

Mehta RV, Upadhyay RV, Charles SW, Ramchand CN (1997) Direct binding of protein to magnetic particles. Biotechnol Technol 77:493–496

Mikhailik OM, Fedorenko OM, Mikhailova SS, Povstugar VI, Lyakhovich AM, Kurbatova GT, Shklovskaya NI, Chuiko AA (1991) Surface structure of finely dispersed iron powders III. Structure of a γ-aminopropyltriethoxysilane-modified coating. Colloids Surf 52:331–338

Newkome GR, Moorefield CN, Vögtle F (2001) Dendrimers and dendrons: concepts syntheses, applications. Wiley-VCH, New York

Ngomsik A, Bee A, Draye M, Cote G, Cabuil V (2005) Magnetic nano- and microparticles for metal removal and environmental applications: a review. C R Chimie 8: 963–970

Norton L, Baskaran K, McKenzie ST (2004) Biosorption of zinc from aqueous solutions using biosolids. Adv Environ Res 8:629–635

Pan BF, Gao F, Gu HC (2005) Dendrimer modified magnetic nanoparticles for protein immobilization. J Colloid Interface Sci 284:1–5

Sun YP (2006) Dispersion of nanoscale iron particles. Ph.D. Dissertation, Lehigh University, United States

United States Environmental Protection Agency Title 40, Code of Federal Regulations (CFR), 2001 revision, Part 143, National Secondary Drinking Water Regulations

Van der Bruggena B, Mänttäri M, Nyström M (2008) Drawbacks of applying nanofiltration and how to avoid them: a review. Sep Purif Technol 63:251–263

Vassilev K, Ford WT (1999) Poly (propylene imine) dendrimer complexes of Cu(II), Zn(II), and Co(III) as catalysts of hydrolysis of p-nitrophenyl diphenyl phosphate. J Polym Sci Part A 37:2727–2736

Wapner K, Grundmeier G (2005) Spectroscopic analysis of the interface chemistry of ultra-thin plasma polymer films on iron. Surf Coat Technol 200:100–103

World Health Organization (WHO) (2003) Zinc in drinking-water

Xu Y, Zhao D (2005) Removal of copper from contaminated soil by use of poly (amidoamine) dendrimers. Environ Sci Technol 39:2369–2375

Xu Z, Liu Q, Finch JA (1997) Silanation and stability of 3-aminopropyl triethoxy silane on nanosized superparamagnetic particles. I. Direct silanation. Appl Surf Sci 120:269–278

Yavuz CT, Mayo JT, Yu WW, Prakash A, Falkner JC, Yean S, Cong L, Shipley HJ, Kan A, Tomson M, Natelson D, Colvin VL (2006) Low-field magnetic separation of monodisperse Fe_3O_4 nanocrystals. Science 314:964–967

Ye L, Pelton R, Brook MA (2007) Biotinylation of TiO_2 nanoparticles and their conjugation with streptavidin. Langmuir 23:5630–5637

Yuan C, Lien H-L (2006) Removal of arsenate from aqueous solution using nanoscale iron particles. Water Qual Res J Can 41:210–215

Zeng F, Zimmerman SC (1997) Dendrimers in supramolecular chemistry: from molecular recognition to self-assembly. Chem Rev 97:1681–1712